THE JOURNAL OF BIOLOGICAL CHEMISTRY
Vol. 277, No. 33, Issue of August 16, pp. 30023–30030, 2002
Printed in U.S.A.

Mutations in the Rho Transcription Termination Factor That Affect RNA Tracking*

Received for publication, November 16, 2001, and in revised form, May 23, 2002
Published, JBC Papers in Press, May 28, 2002, DOI 10.1074/jbc.M111009200

Yi Xu‡, Harold Kohn§, and William R. Widger‡¶

From the ‡Department of Biology and Biochemistry, University of Houston, Houston, Texas 77204-5001 and the §Division of Medicinal Chemistry and Natural Products, School of Pharmacy, University of North Carolina, Chapel Hill, North Carolina 27599-7360

Model studies have identified 16 conserved positively charged amino acids that form a positive strip pointing toward the center hole of Rho. Fourteen residues were individually changed to either an alanine or a glycine and one to a glutamate. Residues Arg^{269}, Arg^{272}, Lys^{283}, Arg^{296}, Lys^{298}, and Arg^{299} form a subdomain (locus) located N-terminal to (above) the ATP hydrolysis domain (P-loop) and mutations in these residues led to either inactive Rho or to proteins displaying decreased k_{cat} for poly(C)-dependent ATP hydrolysis, increased K_m for ribo$(C)_{10}$ activation, and decreased transcription termination efficiencies (57–77%) compared with wild-type Rho. Residues Arg^{347}, Lys^{348}, Lys^{352}, and Arg^{353} form a subdomain (locus) C-terminal to (below) the ATP hydrolysis domain, and mutations in these residues also show a decreased k_{cat} for poly(C)-dependent ATP hydrolysis, an increased K_m for ribo$(C)_{10}$ activation, and a 50–70% decrease in transcription termination, compared with wild-type Rho. Residues Arg^{212} and Lys^{336} surround the ATP hydrolysis domain, and mutations in these residues also altered the kinetic properties of Rho. We conclude that the secondary RNA-tracking site consists of amino acids whose putative orientation faces the central hole in Rho and in part reside in two clusters of positively charged residues located above and below the ATP hydrolysis domain.

Rho transcription termination factor is one of several nucleic acid-binding proteins belonging to a family of helicases with a homohexameric structure shaped like a toroid ring that utilizes the hydrolysis of ATP to move along the nucleic acid (1, 2). Rho protein binds to a poorly defined cytosine-rich sequence on nascent RNA called a *rut* site (Rho utilization), which contains little or no secondary structure. *Rut* sites are usually found upstream from the start of specific genes or between genes in operons (3), and once Rho binds to the *rut* site, it tracks 5′ to 3′ toward the stalled RNA polymerase. In a poorly defined mechanism that may require helicase activity (4), Rho disrupts the polymerase-transcript complex, thereby terminating transcription. Bicyclomycin, a commercial antibiotic, has been shown to inhibit Rho function (5) specifically by interfering with the tracking of Rho (6). Bicyclomycin inhibits the growth of many Gram-negative organisms, including *Escherichia coli*, *Shigella*, and *Salmonella* (7) and at least one Gram-positive bacterium, *Micrococcus luteus* (8), inferring the vital nature of Rho for cellular function (9–11).

The Rho monomer consists of 419 amino acid residues divided into two structural domains, a primary RNA-binding domain (residues 1–151) and the ATP hydrolysis domain (residues 167–419), which is based upon structural similarity with F_1-ATP synthase (12). The RNA-binding domain contains a DGFGFLR (amino acid residues 60–66) conserved RPN-1 RNA recognition motif (13, 14). A solution structure of the N-terminal 130 residues of Rho has been solved using NMR techniques (15) and a crystal structure is also available (16). The primary RNA-binding domain sits as a cap on the toroid ring, distinct from the ATP hydrolysis domain, and binds RNA tightly. ATPase activity is induced by the addition of poly(C) to Rho. Substitution of poly(dC) for poly(C) leads to tight Rho binding but no ATP hydrolysis. The addition of short oligoribonucleotides (7–10 residues long with a predominance of cytosine residues) to the Rho-poly(dC) complex activates ATPase activity. The activation by ribo$(C)_{10}$ is thought to occur at the secondary RNA-binding/tracking site (3).

Recently, the projected Q-loop region, positioned on top, inside the toroid ring, facing the central hole of Rho, has been implicated in RNA binding, and this RNA-binding domain changes conformation upon binding ATP (17). A model for Rho tracking coupled to ATP hydrolysis that relies on the structural similarity between Rho and the β-subunit of F_1-ATP synthase and utilizes residues facing inside of the central hole in Rho has been put forth (18). A strip of positively charged amino acids on Rho positioned toward the inside of the hole was identified based on the structure of bovine F_1-ATP synthase (12, 19) threaded with *E. coli* Rho sequence and energy minimized (18). This model takes into account three active ATP hydrolysis sites per hexamer, sequential hydrolysis of ATP, Rho activation by short oligoribonucleotides, and the discrimination between hydrolytic and inactive subunits. The strip of positive charges was projected to bind the polyphosphate backbone of the RNA as Rho translocates toward the RNA polymerase. The positive charges were clustered into two separate loci found near the N and C termini surrounding the ATP hydrolysis domain. In this paper, we report the effects of site mutations carried out on these amino acid residues. We document the importance of positive charges for Rho to hydrolyze ATP, to bind RNA, and to terminate transcripts.

EXPERIMENTAL PROCEDURES

Materials and Enzymes—Bicyclomycin was kindly provided by Fujisawa Pharmaceutical Co., Ltd. (Osaka, Japan) and was further purified by three successive silica gel chromatographies using 20% methanol-chloroform as the eluant (20). Oligonucleotide primers were synthesized

* This work was supported by U.S. Public Health Service, National Institutes of Health Grant GM37934 (to H. K. and W. R. W.) and Robert A. Welch Foundation Grant E1381 (to W. R. W.). The costs of publication of this article were defrayed in part by the payment of page charges. This article must therefore be hereby marked "*advertisement*" in accordance with 18 U.S.C. Section 1734 solely to indicate this fact.

¶ To whom correspondence should be addressed: Department of Biology and Biochemistry, 369 Science and Research Building II, University of Houston, Houston, TX 77204-5501. Tel.: 713-743-8368; Fax: 713-743-8351; E-mail: widger@uh.edu.

by Genosys Biotechnology, Inc. (The Woodlands, TX). T4 polynucleotide kinase, T4 DNA ligase, and restriction enzymes were purchased from Promega Co. (Madison, WI). *Pfu* DNA polymerase was obtained from Stratagene (La Jolla, CA). The metal chelating column was from Amersham Biosciences.

Radionucleotides [γ-^{32}P]ATP and [α-^{32}P]CTP (3000 Ci/mmol) were purchased from PerkinElmer Life Sciences, and nucleotides and RNase inhibitors were from Ambion, Inc. (Austin, TX). Polyethylenimine thin-layer chromatography plates used for ATPase assays were purchased from J. T. Baker, Inc. Ribo(C)$_{10}$ was obtained from Oligos Etc. (Wilsonville, OR). All other chemicals were reagent grade.

Generation of Mutant Rho Sequences—The plasmid pET-RhoW that contained wild-type *rho* (19) was used as a template for DNA amplification. Overlapping primers with the desired mutation were used to introduce base changes, as described in the QuikChange™ site-directed mutagenesis kit (Stratagene). The resulting PCR-amplified plasmid DNA was digested with *Dpn*I and transformed into host strain JM109. Isolated plasmid DNA from the transformed cells was sequenced with an Applied Biosystems 377 sequencer using the Big Dye reaction kit to identify sequences with specific site changes. The entire *rho* gene was sequenced to ensure that no other mutations were present in the singly mutated gene.

Expression of Mutant Rho Proteins—One of four expression systems were used to generate soluble and functional mutant Rho proteins: the pET14b expression vector using host strain BL21(DE3)pLysS (T7 polymerase) (Novagen), the pET14b vector in the salt-induced T7 polymerase host BL21SI (Invitrogen), the pBAD33 vector (arabinose induction) using host strain MG1655 (21), and the pET14b vector with the λ host HMS174 expressed by introducing T7 polymerase by transfection with λ phage CE6 (Novagen). For expression using host BL21(DE3)pLysS, HSM174, or BL21SI, the original pET14b vector was used. Expression of mutant Rho using the arabinose promoter in the vector pBAD33 required excising the *Xba*I-*Hin*dIII fragment of the pET14b vector that contained the entire *rho* gene including the upstream SD sequence but shy of the T7 promoter, and ligating it into a similarly digested pBAD33 vector. Recombinant plasmids were transformed into host MG1655, and expression was induced by adding 0.2% arabinose to cells.

To isolate Rho, cells were centrifuged, resuspended, and lysed by the addition of lysozyme (130 μg ml^{-1}) and 0.05% deoxycholate. After brief sonication using a Branson sonicator, the cell debris was removed by centrifugation and the resulting supernatant was placed on a metal chelating column (Amersham Biosciences) bound with Ni^{2+}. After washing, the bound protein Rho was recovered using a linear gradient of 0–0.5 M imidazole. SDS electrophoresis of the isolated Rho showed only one peptide at 47,000 Da. Rho protein was dialyzed against storage buffer and kept at −80 °C until used.

Poly(C)-dependent ATP Hydrolysis Assay—Poly(C)-dependent ATP hydrolysis activity was measured as described previously (19) varying the ATP concentrations from 9.1 to 100 μM. The reactions were initiated by adding 0.5 μCi of [γ-^{32}P]ATP and varying concentrations of ATP to a solution of 40 mM Tris-HCl, pH 7.9, 50 mM KCl, 12 mM $MgCl_2$, 0.1 mM EDTA, 0.1 mM dithiothreitol, 1.4 mg ml^{-1} bovine serum albumin, 40 nM poly(C), and Rho (33 nmol of monomer).

Poly(dC)-Ribo(C)$_{10}$-dependent ATP Hydrolysis Activity—The assays were carried out as described (6) using 200 nM Rho protein monomer. The two different ranges of ribo(C)$_{10}$ concentrations used depended upon the K_m (ribo(C)$_{10}$) values. A range ribo(C)$_{10}$ between 0.7 and 20 μM was used for wild-type Rho, whereas a range of ribo(C)$_{10}$ between 20 and 200 μM was used when the K_m indicated a value much greater than the wild-type. Estimates of K_m were reported for values that exceeded 500 μM because of the limited ribo(C)$_{10}$ concentrations that could be used.

Transcription Termination Assay—Transcription termination assays were carried out using a modified *trp* operon (22), as described (6) with slight modifications. In brief, the reaction was carried out in a 10-μl volume with 200 μM ATP, UTP, and GTP and 20 μM CTP, 7 μCi of [α-^{32}P]CTP, 0.1 pmol of template, 0.4 units/μl RNase inhibitor, 0.01 μg/μl *E. coli* RNA polymerase, and 70 nM Rho protein. Transcription termination was measured in the absence and presence of mutant Rho protein and in the presence of Rho plus 50 μM bicyclomycin. The transcripts were separated and visualized as described (6). Subtracting the digitized background from both the read through and the Rho-terminated transcripts allowed quantitation of the termination reactions. The background from the wild-type Rho was subtracted from all the mutants and the percentage of termination was calculated as the amount of terminated transcripts divided by the amount of read through transcript plus the amount of terminated transcript times 100.

RNA Binding Assays—Trp t′ RNA was made using the *Sal*I linearized pTRP5 plasmid and T7 RNA polymerase. The reaction was carried out in 100 μl of transcription buffer (40 mM Tris-HCl, 15 mM $MgCl_2$, 5 mM dithiothreitol, and 0.5 mg/ml acetylated bovine serum albumin), 1 mM each of ATP, GTP, and UTP, and 24 μM CTP, 250 μCi of [α-^{32}P]CTP, 40 units of RNase inhibitor, and 25 μg of DNA. The reaction was started with 1.4 μg of T7 RNA polymerase. The reaction was incubated at 42 °C for 2 h and another 0.56 μg of enzyme was added and incubated for another 2 h. RNase-free DNase (1 μl) was added and the RNA was purified using a RNeasy™ kit (Qiagen). Purity was determined by urea-PAGE and the RNA concentration was determined by A_{260}. Binding of *trp* t′ RNA was carried out in binding buffer (40 mM Tris-HCl, pH 8.0, 25 mM KCl, 10 mM $MgCl_2$, 0.1 mM dithiothreitol, and 0.1 mM EDTA). Binding reaction was started by adding labeled *trp* t′ RNA to a final concentration of 1.2 nM to Rho varying from 0 to 12 nM (hexamer) and incubating at 25 °C for 10 min, followed by filtration of the binding reaction through an S&S nitrocellulose filter presoaked in 1× binding buffer with 0.1 mg/ml denatured yeast RNA. The filter was washed twice with 0.5 ml of binding buffer, dried briefly, and measured with a scintillation counter (6). The percent of Rho binding RNA was measured at saturating RNA concentrations from the moles of RNA bound to Rho times the binding efficiency of Rho to the filter (24) using published procedures (23) and used to estimate the concentration of binding-active Rho. The L50 value, the concentration of Rho that gives half-maximal retention of *trp* t′ RNA was measured using the binding-active Rho concentrations. The K_{nd} and the nth root of K_{nd} was measured as described (24).

Fluorescence Measurements—The fluorescence of F355W and wild-type Rho was determined using a Cary Eclipse spectrofluorimeter at 100 nM Rho monomer in 40 mM Tris-HCl, pH 7.9, 50 mM KCl, 12 mM $MgCl_2$, 0.1 mM EDTA, and 0.1 mM dithiothreitol. Emission spectra were recorded between 300 and 450 nm by excitation at 280 nm, and the spectra were compared by zeroing at 300 nm.

RESULTS

Studies of RNA-protein interactions show that base stacking, geometric complementarity, and coulombic forces contribute to binding (25, 26). A model defining the Rho secondary RNA-binding/RNA-tracking site was proposed based on the symmetry of Rho subunits and the identification of conserved arginine and lysine residues located on the surface of the central hole of the hexameric Rho assembly (18). The notion that RNA tracking occurred through the central hole of Rho was based on RNA cross-linking experiments (17) and by homology to known helicases (27). A technique referred to alanine scanning, which converts selected residues to alanine (glycine), was applied to conserved arginine and lysine residues in the central hole of Rho. The loss of positively charged amino acid residues on Rho function was assessed by comparing the kinetic properties of the mutated Rho protein with wild-type. We included an additional Rho mutant, F355W, in our study to further verify the Rho model. Residue Phe^{355} was homologous to βTyr^{331} in *E. coli* F_1-ATP synthase. Residue βTyr^{331} has been implicated in ATP binding (28) and was base stacked with the adenosine moiety of ATP (29). Accordingly, the replacement of the phenylalanine 355 moiety in Rho with tryptophan provides a potential fluorescence probe sensitive to ATP binding.

Generation of Rho Mutants—The plasmid pET-RhoW (19), which expresses wild-type Rho with a N-terminal His tag using a pET14b vector with a T7 RNA polymerase system, was used as a template for introducing site mutations. Table I summarizes the residues changed and the effect change had on mutant protein expression in various expression systems. The mutant proteins were first expressed from pET14b in the hosts BL21(DE3)pLysS or BL21SI (salt-induced host). Of the 15 mutants in which positively charged amino acids were replaced, only R212G, R347G, K348A, and wild-type grew in the salt-induced host expression strain. The induction of R347G and K348A with isopropyl-1-thio-β-D-galactopyranoside in BL21(DE3)pLysS caused a pronounced decrease in the growth of the cells. This observation suggested that these specific Rho mutations had a negative effect on cell growth. The remaining

TABLE I
Summary of mutations and protein expression

Rho	Locus	Base change	Expression system	Activity
Wild-type			pET14b-BL21pLysS	+
R160A	C-terminal	CGC to GCC	pET14b-λCE6-HMS174	−
R212G	N-terminal	CGT to GGT	pET14b-BL21pLysS	+
R238A	N-terminal	CGC to GCC	pET14b-λCE6-HMS174	+
R269A	N-terminal	CGT to GCT	pET14b-λCE6-HMS174	−
R272A	N-terminal	CGC to GCC	pET14b-λCE6-HMS174	−[a]
K283E	N-terminal	CGC to GCC	pET14b-λCE6-HMS174	−
R296A	N-terminal	CGT to GCT	pET14b-λCE6-HMS174	+
K298A	N-terminal	AAA to GCA	pBAD33-MG1655	+
R299A	N-terminal	CGC to GCC	pBAD33-MG1655	+
K336A	N-terminal	AAA to GCA	pBAD33-MG1655	+
R347G	C-terminal	CGT to GGT	pET14b-BL21pLysS	+
K348A	C-terminal	AAG to GCG	pET14b-BL21SI	+
K352A	C-terminal	AAA to GCA	pBAD33-MG1655	+
R353A	C-terminal	CGC to GCC	pET14b-λCE6-HMS174	+
R384A	C-terminal	CGC to GCC	pET14b-λCE6-HMS174	−[a]
F355W	C-terminal	TTC to TGG	pET14b-BL21SI	+

[a] Expression resulted in the formation of insoluble inclusion bodies.

mutations, when introduced into the BL21 strains, generated few, if any, transformants and those that grew produced truncated protein although the plasmid was stable in host JM109 (data not shown).

Expression from the pBAD33 vector under the arabinose promoter was generally under tighter control (21). The *Xba*I-*Hin*dIII fragment containing the entire *rho* gene from the pET14b was placed in pBAD33, transformed into host MG1655, and expression was induced by adding 0.2% arabinose. Expression of K352A, K298A, and R299A were obtained using the pBAD33 vector. The remaining mutants either did not grow when pBAD33 was transformed into MG1655 or did not express protein. Transforming vectors into the λ host strain HSM174, which lacked T7 RNA polymerase, and inducing expression with λ phage CE6 accomplished expression of the remaining mutant proteins from pET14b vectors R160A, R238A, R269A, R272A, K283E, R296A, R353A, and R384A. Individual colonies were grown in LB media containing 0.2% maltose and ampicillin to 0.6–1.0 A_{600}. Expression was induced by the addition of $2–4 \times 10^9$ plaque-forming units ml^{-1} λ phage CE6 containing the gene for the T7 RNA polymerase. Three h after infection, cells were harvested, lysed, and Rho-purified using the HiTrap metal chelating column bound with Ni^{2+}. These mutants overexpressed protein; however, R160A, R269A, and K283E exhibited no poly(C)-dependent ATPase activity and R272A and R384A produced inclusion bodies that could not be solubilized.

Poly(C)-dependent ATP Hydrolysis Activity—The poly(C)-dependent ATPase activity for the Rho mutants was measured as a function of ATP concentrations (Table II). All of the mutant proteins exhibited a decrease in k_{cat} for ATP hydrolysis when compared with wild-type. Wild-type k_{cat} was 2380 min^{-1}, and only R296A approached this value at 2000 min^{-1}. The other mutants showed k_{cat} values one-half or less of wild-type. Three mutants (R160A, R269A, and K283E) were partially soluble but had no ATP hydrolysis activity. The K_m for His-tagged wild-type was ~5-fold higher than we reported for wild-type Rho (20). This value was consistently observed throughout these experiments. Wild-type Rho exhibited a $K_{m(ATP)}$ of 57 μM, whereas the remaining mutants had either similar (R296A, R299A, K352A, and R353A) or lower (R212G, R347G, and K348A) K_m values ranging from 14 to 36 μM, except for K336A, which gave a $K_{m(ATP)}$ of 125 μM. With the exception of R296A and K336A, amino acid changes at these positions did not adversely affect ATP binding but substantially affected ATP hydrolysis.

The mutations R347G, K348A, K352A, R353A, and F355W were clustered on or near the H-helix close to the adenosine-binding site for ATP. Mutations R347G, K348A, K352A, and R353A showed a 50–90% loss in k_{cat} for poly(C)-dependent ATP hydrolysis, whereas the K_m for ATP was similar to or lower than wild-type.

Poly(dC)-Ribo(C)$_{10}$-stimulated ATP Hydrolysis—ATP hydrolysis rates are induced by binding RNA at the secondary binding/tracking site (3, 19, 30). Amino acid substitutions that alter RNA binding at the secondary/tracking site were expected to alter the kinetics of ATP hydrolysis. RNA activation of ATP hydrolysis activity was determined by varying the ribo(C)$_{10}$ concentrations in the presence of saturating concentrations of poly(dC) and ATP. Most mutant proteins exhibited decreased k_{cat} values compared with the wild-type value of 850 min^{-1} (Table II), and the decrease in the k_{cat} for ribo(C)$_{10}$ activation generally mirrored the k_{cat} values determined in the poly(C)-dependent ATPase assay. Of significance, R296A, K348A, and K352A showed k_{cat} values similar with wild-type. The K_m(ribo(C)$_{10}$) values were sensitive to alanine screening. The K_m(ribo(C)$_{10}$) for wild-type Rho was 9.0 μM. The K336A mutation showed no detectable poly(dC)-ribo(C)$_{10}$-stimulated ATP hydrolysis activity, and the poly(C)-dependent ATPase activity was diminished nearly 18-fold. This was the only mutation with a large increase in the $K_{m(ATP)}$, suggesting that Lys^{336} has a direct role in ATP binding. This finding supports the notion that residues from neighboring subunits can influence ATP binding across the subunit interface (31).

By comparison, most of the active mutants exhibited K_m(ribo(C)$_{10}$) values 5–100-fold greater than wild-type Rho, with the only exception being R347G, which had a K_m(ribo(C)$_{10}$) value of 5.6 μM. R296A and K352A stand out as unusual, the k_{cat} for poly(dC)-ribo(C)$_{10}$-dependent ATP hydrolysis exceeded that of wild-type yet the K_m for ribo(C)$_{10}$ was 500 and 1000 μM, respectively, which was 50–100-fold greater than wild-type Rho. A large increase in the K_m(ribo(C)$_{10}$) coupled with a slight increase in k_{cat} for ATP hydrolysis suggest that the on-rate for ribo(C)$_{10}$ was lower. To support this notion transcription termination efficiencies should be considerably less for these mutants than for wild-type.

Transcription Termination—In vitro transcription termination reactions were measured using the modified *trp* operon fragment (22), as reported (6). Fig. 1*A* shows the transcription termination reactions of wild-type Rho, R212G, R296A, K298A, and R299A, which are located at the putative N-terminal locus of the RNA tracking site. *Lane 12* shows the run-off transcript (labeled *A* in Fig. 1*A*) in the absence of Rho; *lane 1* shows the transcripts in the absence of Rho but with the inclusion of 28

TABLE II
Kinetic paramaters of mutant Rho proteins

Rho	Poly(C)-dependent ATPase		Ribo(C_{10})-dependent ATPase		Termination efficiencies
	K_m(ATP)	k_{cat}	K_m(Ribo($C)_{10}$)	k_{cat}	
	μM	min^{-1}	μM	min^{-1}	%
Wild-type	57	2380	9	850	100
R212G	15	266	333	435	14
R238A	25	167	410	37	
R296A	54	2000	500	1110	53
K298A	36	444	54	100	32
R299A	57	833	333	154	23
K336A	125	133			0
R347G	14	208	5.6	161	41
K348A	14	222	286	800	30
K352A	54	1000	1000	1000	50
R353A	42	588	12	312	97

μM rifampicin, *lane 2* shows transcript produced in the presence of wild-type Rho, and *lane 3* shows the effect of 50 μM bicyclomycin on wild-type Rho. Transcription termination efficiencies as a percentage of wild-type Rho for the mutant proteins as depicted in Fig. 1, *A* and *B,* are summarized in Table II. Mutant R212G generated only 14% of the terminated transcripts compared with wild-type Rho, whereas mutants R296A, K298A, and R299A generated 53, 32, and 23% terminated transcripts, respectively. The terminated transcripts for the mutants were longer than those seen for wild-type Rho. The terminated transcripts are labeled *1*, *2*, and *3* in Fig. 1*A*. Wild-type Rho produced terminated transcripts dominated by 2 and 3 with a small amount of 1. The mutant Rho proteins predominantly produced the longer terminated transcripts 1 and 2 but little, if any 3, the shortest terminated transcript. The production of longer terminated transcripts was reminiscent of the intermediate-size transcripts seen in the titration of Rho with the antibiotic bicyclomycin (6) and the transcripts generated from bicyclomycin-resistant Rho mutants (6). We previously concluded that bicyclomycin slowed the 5′ to 3′ translocation of Rho down the RNA, allowing the RNA polymerase to proceed further along the DNA before transcription termination. A similar argument can be made for the effects of amino acid substitution on transcription termination.

Fig. 1*B* shows transcription termination from mutations (R347G, K348A, K352A, and R353A) clustered on the C-terminal RNA tracking locus. Mutants R347G, K348A, and K352A generated 50% or less terminated transcripts than wild-type, and the terminated transcripts were longer. The mutant R353A showed 97% transcription termination efficiency and gave predominantly larger terminated transcripts than seen for wild-type Rho. This mutant was of interest because the k_{cat} for ATP hydrolysis was between one-third and one-fourth that of wild-type but transcription termination efficiency was not affected. The rate of ATP hydrolysis did not correlate well with transcription termination efficiency. We found a better correlation between the termination efficiency and the K_m(ribo($C)_{10}$) value in the poly(dC)-ribo($C)_{10}$ assay. Bicyclomycin effectively inhibited mutant Rho proteins as seen in Fig. 1. Also, the kinetics of Rho inhibition by bicyclomycin was measured as a function of ATP concentrations using the poly(C)-dependent ATPase assay and we observed that the K_i for bicyclomycin was not altered (data not shown).

RNA Binding Experiments—The binding of *trp* t′ RNA to Rho mutants was measured to determine whether amino acid substitutions at putative secondary RNA-binding/tracking sites affected RNA binding at the primary site. Fig. 2 shows the binding curves and the percent Rho binding RNA for several mutants and the data is summarized in Table III. The filter binding efficiency (23) for wild-type Rho was determined to be very close to unity. Because of the complexity of the binding, the data was analyzed by three separate methods. The simplest was the L50 value, which was the concentration of Rho that gives half-maximal retention of *trp* t′ RNA. Several mutants showed sigmoidal behavior upon RNA binding, and the Hill constants for sigmoidal binding (determined from the slope of the Hill plot at the corresponding L50 value) varied between 1.9 and 4.4 similar to that reported (28). The K_{nd} values were calculated using Equation 2 from Ref. 24 and the Hill constants were as described in Table III. Finally, the nth root of K_{nd} was determined. Wild-type Rho showed the tightest binding with a L50 of binding occurring at 0.81 ± 0.03 nM, whereas the weakest binding mutant, K298A, showed a L50 of >9.0 nM. The L50 values for the other mutants fell within a range of 1.8 to 3.6 nM. Binding of *trp* t′ to R296A, K298A, R353A, and K348A showed binding efficiencies near 50%. Data presented in Table III suggested that mutations distant from the known primary binding site influence tight RNA binding only slightly but may have weakened the hexamer formation in the absence of RNA.

Fluorescence—Fig. 3 shows the fluorescence emission spectra of F355W and wild-type Rho in the absence and presence of 100 μM ATP. We observed that in proceeding from wild-type to F355W, the emission maximum shifted from 375 to 350 nm and increased in emission intensity in the absence of ATP. This emission intensity increase was because of the additional tryptophan residue in the F355W mutant, an increase from one to two tryptophan residues. The blue shift suggests that the additional tryptophan residue was in a solvent inaccessible location in Rho consistent with its predicted placement. The addition of 100 μM ATP caused a 74% decrease in the fluorescence intensity of F355W at 350 nm. By comparison, less than 10% of the fluorescence intensity of wild-type Rho was quenched at 350 nm upon ATP (100 μM) addition. These data provided strong evidence that Phe^{355} is close to the adenosine-binding site, in agreement with the generated structural model for Rho based on the crystal structure of F_1-ATP synthase (32). The relative amount of fluorescence quenching upon ATP addition was greater than that seen for F_1-ATP synthase, presumably because F355W Rho has only one other tryptophan residue.

DISCUSSION

The secondary RNA-binding/tracking site is poorly defined, and only a few mutations with phenotypes consistent with defects in tracking have been identified. Mutations (K352E (30), M327T (33), and E342G (33)) altering ribo($C)_{10}$ binding to Rho have been isolated. Many mutants have decreased k_{cat} for ATP as measured by poly(C)-stimulated ATP hydrolysis. The positions of these mutations are distant from the ATP hydrolysis pocket and are scattered on the inside face of the hexamer (33). We have proposed a structural model of Rho based on the crystal structure of F_1-ATP synthase (18) where the secondary tracking site lies within the central hole, and have provided

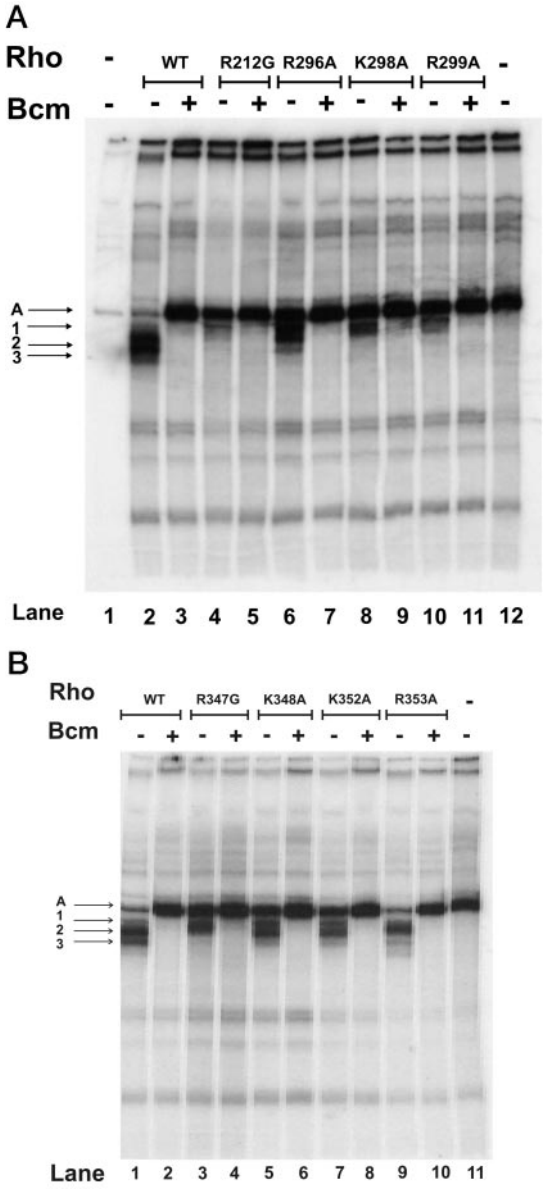

FIG. 1. *A*, transcription termination mediated by Rho mutants clustered in the N-terminal locus of the proposed tracking site. *Lane 1*, reaction carried out in the presence of 28 μM rifampicin without Rho or bicyclomycin; *lane 2*, transcription termination carried out in the presence of 70 nM Rho hexamer; *lane 3*, transcription termination carried out in the presence of 70 nM Rho hexamer in the presence of 50 μM bicyclomycin. *Lanes 4*, *6*, *8*, and *10*, transcription termination carried out in the presence of 70 nM R212G, R296A, K298A, and R299A mutant Rho hexamers, respectively, without bicyclomycin, and *lanes 5*, *7*, *9*, and *11*, transcription termination carried out in the presence of 70 nM R212G, R296A, K298A, and R299A mutant Rho hexamers, respectively, in the presence of 50 μM bicyclomycin. *Lane 12*, transcription termination reaction in the absence of Rho without rifampicin and bicyclomycin. The transcript labeled *A* is the run-off transcript; transcripts *1*, *2*, and *3* are progressively shorter terminated transcripts. The more efficient Rho is the shorter the transcripts. *B*, transcription termination mediated by Rho mutants clustered in the C-terminal locus of the proposed tracking site. *Lane 1*, transcription termination carried out in the presence of 70 nM Rho hexamer; *lane 2*, transcription termination carried out in the presence of 70 nM Rho hexamer in the presence of 50 μM bicyclomycin. *Lanes 3*, *5*, *7*, and *9*, transcription termination carried out in the presence of 70 nM R347G, K348A, K352A, and R353A mutant Rho hexamers, respectively, without bicyclomycin, and *lanes 4*, *6*, *8*, and *10*, transcription termination carried out in the presence of 70 nM R347G, K348A, K352A, and R353A mutant Rho hexamers, respectively, in the presence of 50 μM bicyclomycin. The transcript labeled *A* is the run-off transcript, whereas transcripts *1*, *2*, and *3* are progressively shorter terminated transcripts. *Lane 11*, transcription termination reaction in the absence of Rho and bicyclomycin.

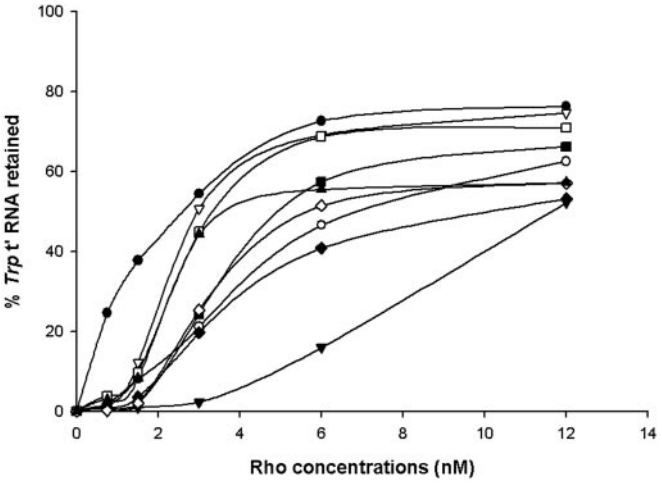

FIG. 2. ***Trp* t′ RNA binding to mutant Rho proteins.** Binding of *trp* t′ RNA at the primary RNA recognition site was compared among the mutant Rho proteins with mutations affecting RNA binding at the RNA-tracking site. All samples contained 1.2 nM ^{32}P-labeled *trp* t′ RNA and the indicated concentrations of Rho (hexamer) in the absence of adenosine nucleotides, wild-type Rho (●), R296A (○), K298A (▼), K352A (▽), R353A (■), F355W (□), R212G (♦), R347G (◇), and K348A (▲).

experimental data to support this hypothesis (34). Moreover, we have identified positively charged amino acids on the inside face of the central hole that can be subdivided into two separate loci.

Enzymatic Activities—Three enzymatic activities helped characterize the mutant and wild-type Rho proteins. Poly(C)-dependent ATP hydrolysis measured the ability of poly(C) to activate Rho-dependent ATP hydrolysis. Poly(C) binds strongly to both the primary and secondary binding sites providing maximum ATP hydrolysis rates. In this assay, the ATP concentrations were varied, whereas poly(C) was maintained at saturating levels. The $K_{m(ATP)}$ value was usually insensitive to parameters affecting RNA binding, whereas the k_{cat} for ATP hydrolysis reflected activation by RNA binding at the tracking site. Because poly(C) binds tightly to both primary and secondary binding sites, this assay is not an effective measure of Rho-RNA interactions necessary for Rho translocation. RNA binding interactions at the tracking site can be determined by measuring the poly(dC)-ribo$(C)_{10}$-dependent ATP hydrolysis activity as a function of ribo$(C)_{10}$ concentration. Both k_{cat} for ATP hydrolysis and K_m(ribo$(C)_{10}$) are indicators of altered RNA binding at the tracking site. Transcription termination is the most sensitive indicator of overall Rho function, exceeding ATP hydrolysis activity. For example, the inhibitor, bicyclomycin, has an I_{50} value for poly(C)-dependent ATP hydrolysis of 60 μM, whereas the transcription termination I_{50} value for bicyclomycin was 5 μM (19). Anti-termination was achieved by slowing the tracking rate such that Rho cannot catch the RNA polymerase, and under these conditions ATP hydrolysis may only be marginally affected. This kinetic coupling model suggests that small changes in ATP hydrolysis may not be responsible for large increases in anti-termination.

Trp t′ RNA Binding—The *trp* t′ RNA binding measured whether the selected mutations adversely altered recognition at the *rut* (primary binding) site contributing to the dominant-negative behavior during mutant protein overexpression. The dominant-negative effect can be reasoned as mutant Rho competing with background wild-type for *rut* sequences. The L50 or *n*th root of K_{nd} for *trp* t′ binding was not significantly altered by these mutations (Table III). This data suggests that *rut* site recognition was not an important factor in the phenotype of the

TABLE III
Trp t′ RNA binding to mutant Rho proteins

L50 is the concentration of Rho that gives half-maximal retention of *trp* t′RNA, the K_{nd} values were derived from Equation 2 ([24]), $fR=(e[L]^n)/(K_{nd}+[L]_n)$.

Rho	L50(nM_{hex})	% Rho binding	K_{nd}(nM_{hex})	Hill constant	K_d (nM_{hex})[a]
Wild-type	0.81 ± 0.03	100	1.21 ± 0.14	1.0	1.20 ± 0.15
R296A	3.56 ± 0.24	50	5.49 ± 0.31	1.9	2.57 ± 0.34
K298A	9.11 ± 0.13	46	81.12 ± 6.17	2.7	5.12 ± 0.07
K352A	1.83 ± 0.01	90	5.92 ± 0.1	2.5	2.09 ± 0.14
R353A	2.94 ± 0.16	44	5.50 ± 1.2	4.1	1.52 ± 0.12
R212G	3.44 ± 0.26	90	48.7 ± 13.8	2.6	4.46 ± 0.17
R347G	2.46 ± 0.30	60	13.79 ± 4.2	4.4	1.84 ± 0.23
K348A	1.86 ± 0.01	44	1.24 ± 0.03	3.7	1.07 ± 0.02
F355W	1.93 ± 0.11	87	7.94 ± 0.65	3.0	2.02 ± 0.08

[a] K_d is the nth root of K_{nd}.

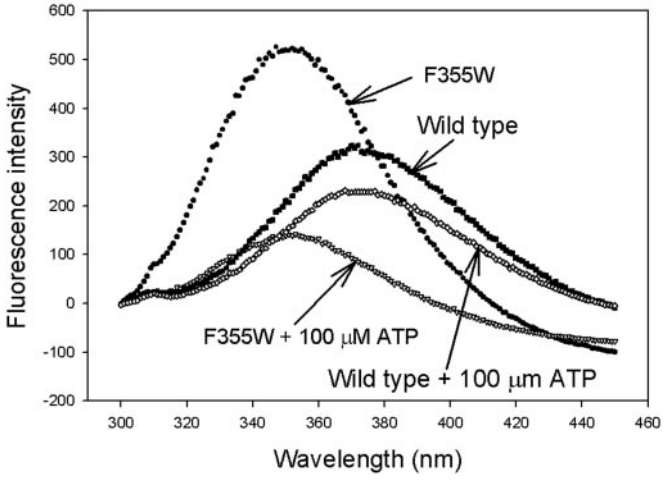

FIG. 3. **Fluorescence emission spectra of wild-type and F355W Rho proteins.** Rho concentrations were 100 nM, and the spectra were recorded using an excitation wavelength of 280 nm in the absence and presence of 100 μM ATP.

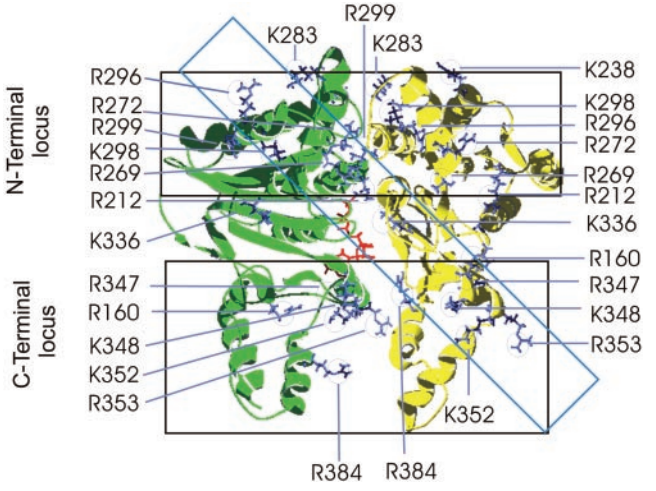

FIG. 4. **A dimeric model of Rho based upon the crystal structure of an α and β subunit pair of F_1-ATP synthase (29) threaded to the Rho sequence and energy minimized as described (18).** This figure shows only residues 151–419 including the ATP binding and hydrolysis pocket; the primary RNA recognition domain, residues 1–150, has been removed. *Outlined* in *black boxes* are two putative secondary RNA (tracking) loci facing the central hole or Rho; positively charged residues altered by site mutations are identified in *blue* and placed in a *rectangle box*. The *green* subunit is depicted as binding ATP (*red*), whereas the *yellow* strand is depicted as not binding ATP.

mutation. These binding experiments were done in the absence of adenosine nucleotides, which are reported to increase RNA binding affinity to Rho (24). However, decreased total RNA binding (percent Rho binding RNA) was seen for several mutants raising the possibility that hexamer formation was weakened in the absence of RNA. R296A showed 50% less *trp* t′ RNA binding, however, this mutant also showed a higher k_{cat} for poly(C)-dependent ATP hydrolysis than wild-type. This suggests that hydrolysis activity was insensitive to small differences in the L50 for *trp* t′ binding. Whereas *trp* t′ binding was a measure of the primary RNA binding affinity, the K_m for ribo$(C)_{10}$ was a better measure of RNA binding to the secondary site. Most of the mutants were defective in transcription termination and displayed large increases in the K_m for ribo$(C)_{10}$. These findings suggested that the mutations were acting at the secondary RNA-binding site primarily and the dominant negative phenotype arose from the slower tracking rates (poorer RNA binding at the secondary RNA-binding site) in the mutant Rho proteins rather than the initial binding step of mutant Rho protein to the *rut* sequences. Slower tracking results in decreased termination and ultimately in cell death.

The Model—Fig. 4 shows a dimeric model of Rho based upon the crystal structure of an α and β subunit pair of F_1-ATP synthase (29) threaded to the Rho sequence and energy minimized as described (18) and shows only residues 151–419 including the ATP binding and hydrolysis pocket; the primary RNA recognition domain, residues 1–150, has been removed. Because the selected mutations can affect Rho at two distinct secondary RNA-binding sites on Rho, we have divided the individual mutants into two groups. We define top as residues next to the N-terminal RNA recognition domain, residues 151–340. The ATP hydrolysis pocket is part of this subdomain including the P-loop residues 181–187 (12) and includes the bicyclomycin binding pocket defined by mutations affecting antibiotic binding (35), residues 219, 266 (5), 210 (8), 208, and 337 (18). The C-terminal or bottom locus, residues 341–419, was located below the ATP hydrolysis domain and contains the adenosine-binding pocket (Fig. 5). Both loci contain positively charged residues, which when altered influence the RNA tracking ability of Rho. The fluorescence quenching of tryptophan emission by ATP (Fig. 3) supports this structural arrangement and our assignment of the ATP-binding domain.

The Top or N-terminal Locus—Residues Arg^{212}, Arg^{238}, Arg^{269}, Arg^{272}, Lys^{283}, Arg^{296}, Lys^{298}, Arg^{299}, and Lys^{336} are found in the N-terminal locus pointing toward the central hole of Rho. Mutations in three of these residues resulted in inactive Rho: R272A formed insoluble inclusion bodies; R269A and K283E were isolated, purified, and shown to have no poly(C)-stimulated ATP hydrolysis activity. Lysine 283 on the Q-loop was also shown to be important in Rho ATP hydrolysis activity (36). R238A, R296A, K298A, and R299A displayed dominant-negative growth suggesting competition with the host wild-type Rho but preventing effective termination. We found that most of the mutant proteins had altered kinetic properties ($K_{m(ATP)}$ and k_{cat}) in the poly(C)-dependent ATPase assay com-

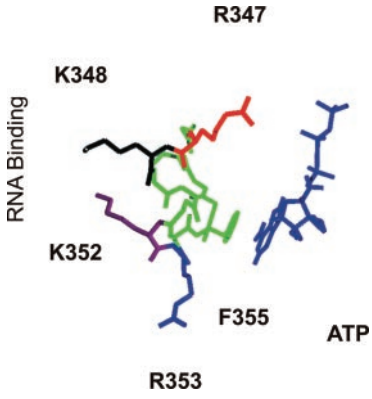

FIG. 5. **A structural model of residues on the putative H-helix based on the structure of F_1-ATP synthase β subunit, where Phe^{355} interacts with the adenosine ring of ATP on one face of the helix and residues Arg^{347}, Lys^{348}, Lys^{352}, and Arg^{353} interact on the other face, presumably binding RNA.**

pared with wild-type Rho. The only exception was R296A, which showed comparable $K_{m(ATP)}$ and k_{cat} values with wild-type Rho. K298A and K299A had k_{cat} of 19 and 35% of wild-type, respectively, whereas the $K_{m(ATP)}$ values were similar to wild-type. R212G and K336A were adjacent to the ATP hydrolysis pocket and showed a large decrease in the turnover number (k_{cat}), 11 and 6%, respectively, compared with wild-type Rho. The $K_{m(ATP)}$ for R212G was lower than wild-type, but the $K_{m(ATP)}$ for K336A was more than double the native enzyme.

Poly(dC)-ribo$(C)_{10}$-stimulated ATPase activity for R296A (K_m = 500 μM) showed a K_m(ribo$(C)_{10}$) more than 50-fold greater than wild-type (K_m = 9 μM), indicating that RNA binding at the secondary site in R296A was weaker than wild-type. Interestingly, there was an increase in the ATP turnover for this mutant from 850 to 1110 min^{-1}. The other N-terminal locus mutants showed elevated K_m(ribo$(C)_{10}$) values ranging from 54 to 410 μM and decreased k_{cat} values ranging from 435 to 37 min^{-1} (Table II). R212G showed a large decrease in turnover for poly(C)-dependent ATPase activity, exceeding the decrease in the turnover number for poly(dC)-ribo$(C)_{10}$ dependent activity. The activity for K336A in the poly(dC)-ribo$(C)_{10}$ dependent assay could not be measured.

Transcription termination was often impaired in mutants that had altered ribo$(C)_{10}$ binding (Table II). R296A acted as a classic uncoupler, where uncoupling was defined as the absence of detectable translocation without the loss of ATP hydrolysis. ATP hydrolysis provides the energy for RNA translocation, and R296A impaired both translocation and transcription termination without interfering with ATP hydrolysis. The rate-limiting step in Rho function is presumably translocation (37), and if this step is circumvented or uncoupled, an increase in ATP hydrolysis could be expected, similar to the increase in electron transport rates when ATP synthesis is uncoupled from electron transport.

As anticipated, the transcription termination efficiencies were affected by the other N-terminal locus mutations (Table II). Most of these mutants showed large decreases in the k_{cat} for ATP hydrolysis, increased K_m(ribo$(C)_{10}$) values, and decreased transcription termination efficiencies. We suggest that amino acid substitution in these mutant Rho proteins disrupted RNA binding at the tracking site and prevented the formation of the catalytically active conformation necessary for ATP hydrolysis. The loss of RNA binding at the N-terminal locus resulted in greatly diminished ATP hydrolysis and greatly reduced transcription termination. Again, R296A is phenotypically different; ATP hydrolysis increased but transcription termination decreased. This finding suggests that in R296A RNA binding is sufficient to promote ATP hydrolysis, but is not tight enough to prevent RNA slippage. The net result is that translocation is ineffective or does not occur and thereby circumvents the rate-determining step. We predict that R296A may show an altered initial presteady-state rate of ATP hydrolysis compared with wild-type Rho (37, 38).

The Bottom or C-terminal Locus—Residues R347G, K348A, K352A, R353A, and R384A in the C-terminal locus, speculated to be involved in Rho-RNA tracking, were selected for study. R347G, K348A, K352A, and R353A are believed to reside in the putative H-helix, which on one face is projected to bind to the adenosine ring of ATP and on the other face to RNA. Fig. 5 shows the positions of these residues in relation to the ATP binding. Two other residues, Lys^{402} and Lys^{407}, were considered promising but were not pursued. Completing our mutational studies for this locus was F355W, which positioned a tryptophan residue near the ATP binding pocket.

R384A and R160A were only expressed as inactive inclusion bodies. Moreover, these inclusion bodies were only generated in the phage-induced expression system, and transformed cells carrying this mutant in the other expression systems failed to grow. The observed dominant-negative phenotype for these mutants suggested a role in RNA tracking.

Mutants R347G, K348A, K352A, and R353A fell into two types, those with K_m(ribo$(C)_{10}$) values similar to wild-type Rho and those with K_m(ribo$(C)_{10}$) values 20–100 times higher. R347G and R353A had similar K_m(ribo$(C)_{10}$) values to wild-type, but their $K_{m(ATP)}$ values were lower than those of native enzyme. The k_{cat} for ATP hydrolysis for R347G and R353A was 9 and 25% of wild-type in the poly(C)-dependent ATPase assay and 19 and 37% for the poly(dC)-ribo$(C)_{10}$-mediated ATPase assay. Transcription termination for R347G was only 41% of wild-type Rho and produced only the largest terminated transcript, whereas R353A activity was almost identical to wild-type Rho and showed only minor differences in the termination pattern (Fig. 1*B*). R353A showed a 3.6-fold increase in the L50 for *trp* t′ RNA binding and only 44% of this Rho bound RNA, but this mutant still effectively terminated transcription and did not have an altered K_m for ribo$(C)_{10}$.

Mutants K348A and K352A showed increased K_m(ribo$(C)_{10}$) values compared with wild-type Rho (K_m(ribo$(C)_{10}$) = 9 μM) at 286 and >1000 μM, respectively. K348A showed a defective k_{cat} for ATP hydrolysis, a decreased $K_{m(ATP)}$ value, and a transcription termination efficiency that was 30% of wild-type. Again, there was a strong correlation between K_m(ribo$(C)_{10}$) and transcription termination efficiency. We found that the k_{cat} for poly(dC)-ribo$(C)_{10}$-dependent ATP hydrolysis was greater than wild-type Rho and that this mutant displayed an overall pattern of inhibition comparable with R296A, showing decreased transcription termination efficiency but increased ATP hydrolysis, which suggests that K352A behaves as an uncoupler.

The *E. coli* F_1-ATP synthase β subunit counterpart of Phe^{355}, βTyr^{331} (28), is base stacked with the adenosine and the tryptophan mutant Y331W shows fluorescence quenching upon ATP binding (32, 28). The Rho F355W mutation decreased the k_{cat} for poly(C)-dependent ATP hydrolysis by only 50%, whereas $K_{m(ATP)}$ increased from 57 to 83 μM. Furthermore, transcription termination was not affected by this amino acid substitution. Fig. 3 shows a blue shift in fluorescence emission maximum from 380 to 350 nm and an increase in total fluorescence compared with wild-type Rho. A large decrease in fluorescence was observed for the F355W mutant upon the addition of 100 μM ATP but not for wild-type. These data suggested that Rho Phe^{355}, like F_1-ATP synthase βTyr^{331}, interacts strongly with ATP.

Fig. 5 shows the orientation of amino acids Arg^{347}, Lys^{348},

Lys^{352}, Arg^{353}, and Phe^{355} with respect to ATP binding. Lys^{348} and Lys^{352} point out of the opposite face of the helix from Phe^{355}, which binds ATP. Losses of positive charges at these residues caused a large increase in the K_m(ribo$(C)_{10}$) for RNA binding at the tracking site. We found that the $K_{m(ATP)}$ for Lys^{348} was smaller than wild-type Rho, suggesting that RNA binding at the C-terminal locus may alter ATP binding. Mutations introduced at Arg^{347} and Arg^{353} did not greatly affect the L50 for *trp* t′ RNA binding and are positioned away from the putative RNA binding face of the H-helix. Arg^{347} is close to the β phosphate of ATP, consistent with the large decreases in the k_{cat} for ATP hydrolysis observed for R347G in the poly(C)-dependent and the poly(dC)-ribo$(C)_{10}$-dependent ATPase assays.

Our model (18) involves alternate binding and release of RNA at two loci in Rho catalyzed by ATP binding, hydrolysis, and ADP release in a sequential mechanism and our data, on the effect site mutations on RNA binding to the tracking site is consistent with this model. Studies are in progress that measure ATP binding to Rho using F355W fluorescence quenching under different ligand binding conditions and the use of double mutants geared to detect alternating RNA and ATP binding.

Acknowledgments—We thank Dr. M. Kawamura and the Fujisawa Pharmaceutical Co. Ltd., Japan, for the gift of bicyclomycin and Thomas Weber for critical discussions and suggestions on experimental design. We are grateful to and Dr. Michael Benedik for helpful discussions about overexpressing Rho protein.

REFERENCES

1. Lohman, T. M., and Bjornson, K. P. (1996) *Annu. Rev. Biochem.* **65,** 169–214
2. Bird, L. E., Subramanya, H. H., and Wigley, D. B. (1998) *Curr. Opin. Struct. Biol.* **8,** 14–18
3. Richardson, J. P. (1982) *J. Biol. Chem.* **257,** 5760–5766
4. Brennan, C. A., Dombroski, A. J., and Platt, T. (1987) *Cell* **48,** 945–952
5. Zwiefka, A., Kohn, H., and Widger, W. R. (1993) *Biochemistry* **32,** 3564–3570
6. Magyar, A., Zhang, X., Kohn, H., and Widger, W. R. (1996) *J. Biol. Chem.* **271,** 25369–25374
7. Williams, R. M., and Durham, C. A. (1988) *Chem. Rev.* **88,** 511–540
8. Nowatzke, W. L., Keller, E., Koch, G., and Richardson, J. P. (1997) *J. Bacteriol.* **179,** 5238–5240
9. Das, A., Court, D., and Adhya, S. (1976) *Proc. Natl. Acad. Sci. U. S. A.* **73,** 1959–1963
10. Inoko, H., Shigesada, K., and Imai, M. (1977) *Proc. Natl. Acad. Sci. U. S. A.* **74,** 1163–1166
11. Richardson, J. P., and Carey, J. L., III (1982) *J. Biol. Chem.* **257,** 5767–5771
12. Dombroski, A. J., LaDine, J. R., Cross, R. L., and Platt, T. (1988) *J. Biol. Chem.* **263,** 18810–18815
13. Martinez, A., Burns, C. M., and Richardson, J. P. (1996) *J. Mol. Biol.* **257,** 909–918
14. Brennan, C. A., and Platt, T. (1991) *J. Biol. Chem.* **266,** 17296–17305
15. Briercheck, D. M., Wood, T. C., Allison, T. J., Richardson, J. P., and Rule, G. S. (1998) *Nat. Struct. Biol.* **5,** 393–399
16. Allison, T. J., Wood, T. C., Briercheck, D. M., Rastinejad, F., Richardson, J. P., and Rule, G. S. (1998) *Nat. Struct. Biol.* **5,** 352–356
17. Wei, R. R., and Richardson, J. P. (2001) *J. Biol. Chem.* **276,** 28380–28387
18. Vincent, F., Openshaw, M., Trautwein, M., Gaskell, S. J., Kohn, H., and Widger, W. R. (2000) *Biochemistry* **39,** 9077–9083
19. Magyar, A., Zhang, X., Abdi, F., Kohn, H., and Widger, W. R. (1999) *J. Biol. Chem.* **274,** 7316–7324
20. Park, H., Zhang, X., Moon, H., Zwiefka, A., Cox, K., Gaskell, S. J., Widger, W. R., and Kohn, H. (1995) *Arch. Biochem. Biophys.* **323,** 447–454
21. Guzman, L.-M., Belin, D., Carson, M. J., and Beckwith, J. (1995) *J. Bacteriol.* **177,** 4121–4130
22. Wu, A. M., Christie, G. E., and Platt, T. (1981) *Proc. Natl. Acad. Sci. U. S. A.* **78,** 2913–2917
23. Witherall, G. W., and Uhlenbeck, O. C. (1989) *Biochemistry* **28,** 71–76
24. Gan, E., and Richardson, J. P. (1999) *Biochemistry* **38,** 16882–16888
25. Burd, C. G., and Dreyfuss, G. (1994) *Science* **265,** 615–621
26. Draper, D. E. (1995) *Annu. Rev. Biochem.* **64,** 593–620
27. Kim, D. E., and Patel, S. S. (2001) *J. Biol. Chem.* **276,** 13902–13910
28. Weber, J., Wilke-Mounts, S., Lee, R. S. F., Grell, E., and Senior, A. E. (1993) *J. Biol. Chem.* **27,** 20126–20133
29. Abrahams, J. P., Leslie, A. G., Lutter, R., and Walker, J. E. (1994) *Nature* **370,** 621–628
30. Pereira, S., and Platt, T. (1995) *J. Mol. Biol.* **251,** 30–40
31. Vincent, F., Widger, W. R., Openshaw, M., Gaskell, S. J., and Kohn, H. (2000) *Biochemistry* **39,** 9067–9076
32. Weber, J., Bowman, C., and Senior, A. E. (1996) *J. Mol. Biol.* **271,** 18711–18718
33. Miwa, Y., Horiguchi, T., and Shigesada, K. (1995) *J. Mol. Biol.* **254,** 815–837
34. Burgess, B. R., and Richardson, J. P. (2001) *J. Biol. Chem.* **276,** 4182–4189
35. Vincent, F., Srinivasan, J., Santillán, A., Jr., Widger, W. R., and Kohn, H. (2001) *J. Org. Chem.* **66,** 2251–2264
36. Wei, R. R., and Richardson, J. P. (2001) *J. Mol. Biol.* **314,** 1007–1015
37. Kim, D. E., Shigesada, K., and Patel, S. S. (1999) *J. Biol. Chem.* **274,** 11623–11628
38. Stitt, B. L., and Xu, Y. (1998) *J. Biol. Chem.* **373,** 26477–26486